Journal of Engineering Mathematics **33:** 77–102, 1998.

Differential-flow-induced instability in a cubic autocatalator system

R.A. SATNOIANU[1,2], J.H. MERKIN[1] and S.K. SCOTT[2]
[1]*Department of Applied Mathematical Studies, University of Leeds, Leeds, LS2 9JT, UK, e-mail: amtjhm@amsta.leeds.ac.uk*
[2]*School of Chemistry, University of Leeds, Leeds, LS2 9JT, UK*

Received 22 October 1996; accepted in revised form 5 August 1997

Abstract. The formation of spatio-temporal stable patterns is considered for a reaction-diffusion-convection system based upon the cubic autocatalator, $A + 2B \to 3B$, $B \to C$, with the reactant A being replenished by the slow decay of some precursor P via the simple step $P \to A$. The reaction is considered in a differential-flow reactor in the form of a ring. It is assumed that the reactant A is immobilised within the reactor and the autocatalyst B is allowed to flow through the reactor with a constant velocity as well as being able to diffuse.

The linear stability of the spatially uniform steady state $(a, b) = (\mu^{-1}, \mu)$, where a and b are the dimensionless concentrations of the reactant A and autocatalyst B, and μ is a parameter reflecting the initial concentration of the precursor P, is discussed first. It is shown that a necessary condition for the bifurcation of this steady state to stable, spatially non-uniform, flow-generated patterns is that the flow parameter $\phi > \phi_c(\mu, \lambda)$ where $\phi_c(\mu, \lambda)$ is a (strictly positive) critical value of ϕ and λ is the dimensionless diffusion coefficient of the species B and also reflects the size of the system. Values of ϕ_c at which these bifurcations occur are derived in terms of μ and λ. Further information about the nature of the bifurcating branches (close to their bifurcation points) is obtained from a weakly nonlinear analysis. This reveals that both supercritical and subcritical Hopf bifurcations are possible. The bifurcating branches are then followed numerically by means of a path-following method, with the parameter ϕ as a bifurcation parameter, for representatives values of μ and λ. It is found that multiple stable patterns can exist and that it is also possible that any of these can lose stability through secondary Hopf bifurcations. This typically gives rise to spatio-temporal quasiperiodic transients through which the system is ultimately attracted to one of the remaining available stable patterns.

Key words: flow reactor, cubic autocatalator, absolute instability, travelling waves, Stuart-Landau amplitude equation.

1. Introduction

The interaction of molecular diffusion with nonlinear kinetics in an initially-uniform reacting chemical system, which is otherwise temporally stable, can lead to the uniform state becoming unstable through a Turing or diffusion-driven instability [1], [2, Sects 14.2, 14.3], [3, Sect. 6.7] and [4, Sect. 2.2]. In its simplest form this instability requires two species, an activator (or autocatalytic species) and an inhibitor (whose role is to limit the autocatalytic growth) and also that the diffusion coefficients of these two species should differ (usually considerably), with that for the inhibitor being larger than that for the activator. The bifurcation from the spatially uniform stationary state though this instability may give rise to pattern formation, *i.e.* to stable, spatially non-uniform configurations of the reaction-diffusion system. The occurrence of these patterns, originally predicted theoretically, has been verified experimentally [5–7]. They can also form the starting point through secondary and higher-order bifurcations, for the development of complex spatio-temporal structures [6, 8–10].

More recently, a reactor has been designed in which the different transport rates for the activator and inhibitor species is achieved by causing these species to flow through the reactor with different velocities [11–13]. This configuration can also give rise to spatially uniform

stationary states of the system becoming unstable through what is termed a differential-flow-induced chemical instability (DIFICI). In this case the new stable structures that arise from this bifurcation are travelling waves of permanent form propagating with constant velocity. The interaction between Turing and DIFICI bifurcations has been shown, [14], to produce complex time dependent spatial structures, including propagating stripes and spots.

Here we consider a model for the differential-flow reactor based on 'cubic autocatalator' kinetics in which a reactant A is formed at a constant rate from some precursor P, via

$$P \to A \quad \text{rate} = \kappa_0 P_0, \tag{1.1}$$

with the reactant A and autocatalyst B reacting further according to the scheme

$$A + 2B \to 3B \quad \text{rate} = \kappa_1 a b^2, \tag{1.2}$$

$$B \to C \quad \text{rate} = \kappa_2 b, \tag{1.3}$$

(where a and b are the concentrations of chemical species A and B, respectively and κ_0, P_0, κ_1 and κ_2 are all constants).

In this paper, we assume further that reactant A is effectively immobilised within the reactor. This might be achieved, for example, by creating the reaction domain as a matrix of small beads, with the reactant A adsorbed into the surface of these. The movement of the autocatalyst B is considered not to be so constrained and this species is made to flow through the reactor with a constant velocity u as well as being able to diffuse (with diffusion coefficient D_B). Note that we therefore have $D_B > D_A$, the opposite of the inequality appropriate to Turing instabilities.

These considerations lead to the reaction-diffusion-advection equations for our model as

$$\frac{\partial a}{\partial t} = \kappa_0 P_0 - \kappa_1 a b^2, \tag{1.4}$$

$$\frac{\partial b}{\partial t} + u\frac{\partial b}{\partial x} = D_B \frac{\partial^2 b}{\partial x^2} + \kappa_1 a b^2 - \kappa_2 b. \tag{1.5}$$

A detailed derivation of these equations (without the flow term) including a validation of the pooled-chemical approximation inherent in Equations (1.1)–(1.4) is given in [15, 16].

We solve Equations (1.4)–(1.5) subject to periodic boundary conditions at the ends of the reaction domain $x = 0$ and $x = l$ and to initial conditions which we leave unspecified for the present. We impose these particular boundary conditions partly for ease in the calculations described below, which enable considerable progress to be made analytically in understanding the basic process involved, and partly for consistency with [14]. They are also not incompatible with our model, since we can regard the reaction domain as forming a part of some larger system in which a moving pattern has been created.

We start by making Equations (1.4)–(1.5) dimensionless and, to do so, we follow [15, 16] by writing

$$a = \left(\frac{\kappa_2}{\kappa_1}\right)^{1/2} \overline{a}, \qquad b = \left(\frac{\kappa_2}{\kappa_1}\right)^{1/2} \overline{b}, \qquad \overline{t} = \kappa_2 t, \qquad \overline{x} = \frac{x}{l}. \tag{1.6}$$

This leads to the dimensionless equations, where bars have been dropped for convenience

$$\frac{\partial a}{\partial t} = \mu - ab^2, \tag{1.7}$$

$$\frac{\partial b}{\partial t} = \lambda \frac{\partial^2 b}{\partial x^2} - \phi \frac{\partial b}{\partial x} + ab^2 - b \tag{1.8}$$

on $0 \leqslant x \leqslant 1, t \geqslant 0$, subject to the boundary conditions

$$\begin{cases} a(0,t) = a(1,t), a_x(0,t) = a_x(1,t), \ldots, \\ b(0,t) = b(1,t), b_x(0,t) = b_x(1,t), \ldots. \end{cases} \tag{1.9}$$

The dimensionless parameters are given by

$$\mu = \frac{\kappa_0 P_0}{\kappa_2} \left(\frac{\kappa_1}{\kappa_2}\right)^{1/2}, \qquad \lambda = \frac{D_B}{\kappa_2 l^2}, \qquad \phi = \frac{u}{\kappa_2 l} \quad \text{(flow parameter)}. \tag{1.10}$$

A system similar to Equations (1.7)–(1.9) (without the flow term and with reactant A being allowed to diffuse) has been studied previously [10, 17] and the conditions for the spatial mode bifurcations to stable patterns were derived. The complex spatio-temporal structures (including travelling waves and modulated travelling waves) which arise through spatial mode interactions have also been determined.

Equations (1.7)–(1.9) have the unique spatially uniform stationary state $S = \{(a,b) = (\mu^{-1}, \mu)\}$ which is temporally stable for all $\mu \geqslant 1$, [15, 16]. Here we are concerned with the study of bifurcations from this stable state to form new stable spatio-temporal patterns as the parameter ϕ (which we treat as our bifurcation parameter) is varied. In particular, we are interested in how the differential flow of reactant and autocatalyst can destabilise S and thus we restrict our attention to the case $\mu \geqslant 1$.

We begin by analysing the linear stability of the uniform steady state S.

2. Linear stability analysis

To determine the system linearized around S and to deduce its spectrum, which is equivalent to finding the dispersion relation, we assume that, at $t = 0$, an initial disturbance of small amplitude is imposed on the system. We represent this by the initial conditions

$$\begin{cases} a(x,0) = \dfrac{1}{\mu} + \delta \overline{a_0}(x) \\ b(x,0) = \mu + \delta \overline{b_0}(x) \end{cases}, \quad 0 \leqslant x \leqslant 1, \tag{2.1}$$

where $\overline{a_0}(x), \overline{b_0}(x)$ are bounded functions on $0 \leqslant x \leqslant 1$ and $0 < \delta \ll 1$ is a measure of the amplitude of the initial disturbance. We look for a solution of Equations (1.7)–(1.9), with the initial conditions (2.1) in the form of

$$\begin{cases} a(x,t) = \dfrac{1}{\mu} + \delta \overline{a}(x,t) + \cdots, \\ b(x,t) = \mu + \delta \overline{b}(x,t) + \cdots, \end{cases} \tag{2.2}$$

where $\overline{a}, \overline{b}$ are of $O(1)$ as $\delta \to 0$.

After making these substitutions in Equations (1.7)–(1.9) and neglecting terms of $O(\delta^2)$, we obtain the linear equations for $\overline{a}, \overline{b}$

$$\frac{\partial \overline{a}}{\partial t} = -\mu^2 \overline{a} - 2\overline{b}, \tag{2.3}$$

$$\frac{\partial \overline{b}}{\partial t} = \lambda \frac{\partial^2 \overline{b}}{\partial x^2} - \phi \frac{\partial \overline{b}}{\partial x} + \mu^2 \overline{a} + \overline{b} \tag{2.4}$$

on $0 \leqslant x \leqslant 1$ and $t \geqslant 0$, subject to the initial and boundary conditions

$$\overline{a}(x,0) = \overline{a_0}(x), \qquad \overline{b}(x,0) = \overline{b_0}(x), \tag{2.5}$$

$$\begin{cases} \overline{a}(0,t) = \overline{a}(1,t), & \overline{a}_x(0,t) = \overline{a}_x(1,t), \dots, \\ \overline{b}(0,t) = \overline{b}(1,t), & \overline{b}_x(0,t) = \overline{b}_x(1,t), \dots . \end{cases} \tag{2.6}$$

Boundary conditions (2.6) suggest that we look for a solution in the form

$$\overline{a}(x,t) = \sum_{n=0}^{\infty} \{a_n(t)\cos(2n\pi x) + b_n(t)\sin(2n\pi x)\}, \tag{2.7}$$

$$\overline{b}(x,t) = \sum_{n=0}^{\infty} \{c_n(t)\cos(2n\pi x) + d_n(t)\sin(2n\pi x)\}. \tag{2.8}$$

When these expressions are substituted in the linearized system (2.3)–(2.4), we obtain the system of linear ordinary differential equations for the Fourier coefficients a_n, b_n, c_n, d_n

$$\begin{cases} \dfrac{\mathrm{d}a_n}{\mathrm{d}t} + \mu^2 a_n + 2c_n = 0, \\ \dfrac{\mathrm{d}b_n}{\mathrm{d}t} + \mu^2 b_n + 2d_n = 0, \\ \dfrac{\mathrm{d}c_n}{\mathrm{d}t} + (k_n^2 - 1)c_n + \gamma_n d_n - \mu^2 a_n = 0, \\ \dfrac{\mathrm{d}d_n}{\mathrm{d}t} + (k_n^2 - 1)d_n - \gamma_n c_n - \mu^2 b_n = 0, \end{cases} \tag{2.9}$$

where $k_n^2 = 4\pi^2 n^2 \lambda$ and $\gamma_n = 2\pi n \phi$. (2.10)

The solution to Equations (2.9) is obtained as

$$\begin{pmatrix} a_n(t) \\ b_n(t) \\ c_n(t) \\ d_n(t) \end{pmatrix} = \begin{pmatrix} A_n \\ B_n \\ C_n \\ D_n \end{pmatrix} \exp(\omega_n t), \tag{2.11}$$

where $\omega_n = \omega_n(k_n, \mu, \phi)$ and A_n, B_n, C_n, D_n are constants (possibly complex). On substituting (2.11) in Equations (2.9), we find a linear algebraic system for the A_n, B_n, C_n, D_n which

has a nontrivial solution, provided each $\omega_n (n = 0, 1, 2, \ldots)$ satisfies a quartic polynomial equation. This gives the dispersion relation, which we can write as

$$(\alpha_n \beta_n + 2\mu^2)^2 + \alpha_n^2 \gamma_n^2 = 0, \tag{2.12}$$

where $\alpha_n = \omega_n + \mu^2$ and $\beta_n = \omega_n + k_n^2 - 1$. The dispersion relation (2.12) can be factorised into

$$\omega_n^2 + (p_n - i\gamma_n)\omega_n + q_n - i\gamma_n \mu^2 = 0, \tag{2.13}$$

$$\omega_n^2 + (p_n + i\gamma_n)\omega_n + q_n + i\gamma_n \mu^2 = 0. \tag{2.14}$$

for all $n \geqslant 0$, where we have written $p_n = k_n^2 + \mu^2 - 1, q_n = \mu^2(k_n^2 + 1) > 0$. We notice that $p_n \geqslant 0, q_n > 0$ for all $n \geqslant 0$ and $p_n = 0$ if and only if $n = 0, \mu = 1$.

If we denote by ω_n^i $(i = 1, 2, 3, 4, \ldots, n = 0, 1, \ldots)$ the four roots of the dispersion relation (2.12) then the solution to the linear initial-boundary value problem (2.3)–(2.6) is readily obtained as

$$\begin{aligned} \overline{a}(x,t) &= \sum_{n=0}^{\infty} \left\{ \left[\sum_{i=1}^{4} A_n^i \exp(\omega_n^i t) \right] \cos(2n\pi x) + \left[\sum_{i=1}^{4} B_n^i \exp(\omega_n^i t) \right] \sin(2n\pi x) \right\}, \\ \overline{b}(x,t) &= \sum_{n=0}^{\infty} \left\{ \left[\sum_{i=1}^{4} C_n^i \exp(\omega_n^i t) \right] \cos(2n\pi x) + \left[\sum_{i=1}^{4} D_n^i \exp(\omega_n^i t) \right] \sin(2n\pi x) \right\}, \end{aligned} \tag{2.15}$$

for $0 \leqslant x \leqslant 1, t \geqslant 0$. Here $A_n^i, B_n^i, C_n^i, D_n^i, (i = 1, 2, 3, 4, n = 0, 1, 2, \ldots)$, are constants related to the Fourier series expansions of the initial perturbation.

We now proceed to examine the dispersion relation in detail.

2.1. THE DISPERSION RELATION

The roots of Equation (2.13) can be expressed as a pair of complex conjugates

$$\omega_n^{1,2} = \sigma_n^{\pm} - i\eta_n^{\mp}, \tag{2.16}$$

where

$$\sigma_n^{\pm} = \frac{1}{2} \left\{ -p_n \pm \frac{1}{\sqrt{2}} [E_n - \gamma_n^2 + [(E_n - \gamma_n^2)^2 + 4\gamma_n^2 (k_n^2 - 1 - \mu^2)^2]^{1/2}]^{1/2} \right\}, \tag{2.17}$$

$$\eta_n^{\pm} = \frac{1}{2} \left\{ -\gamma_n \pm \frac{1}{\sqrt{2}} [\gamma_n^2 - E_n + [(\gamma_n^2 - E_n)^2 + 4\gamma_n^2 (k_n^2 - 1 - \mu^2)^2]^{1/2}]^{1/2} \right\}, \tag{2.18}$$

Here $E_n = p_n^2 - 4q_n$. For Equation (2.14) the two eigenvalues are given by

$$\omega_n^{3,4} = \sigma_n^{\pm} + i\eta_n^{\mp}, \tag{2.19}$$

so that $\overline{\omega}_n^{1,2} = \omega_n^{3,4}$, where the overbar denotes the complex conjugate operator.

It is readily established that

(i) $\eta_0^- \neq 0, \eta_n^{\pm} \neq 0$ (for all $n = 1, 2, \ldots$), except when $\phi = 0$. Note that η_0^+ can be zero for some $\mu > 1$ with

$$E_0 = (\mu^2 - 1)^2 - 4\mu^2 > 0, \tag{2.20}$$

(ii) $$\sigma_n^- < 0, \quad \sigma_n^+ \gtrless 0, \quad \sigma_n^+ > \sigma_n^-, \quad \text{for all } n = 0, 1, 2, \ldots. \tag{2.21}$$

We note that $\sigma_0^+ \neq 0$ for $E_0 > 0$.

From (i) and (ii) we have that ω_n^i, $(i = 1, 2, 3, 4)$ are always complex (for $n > 0$) and that only $\mathrm{Re}\{\omega_n^1\} = \mathrm{Re}\{\omega_n^3\}$ can be positive.

(iii) σ_n^+ has an horizontal asymptote when $\phi \to \infty (\gamma_n \to \infty)$. (2.22)

(iv) for each $n = 0, 1, 2, \ldots$, there is at most one $\phi = \phi_c$ such that

$$\sigma_n^+(\phi_c) = 0 \quad \text{and} \quad \frac{\mathrm{d}\sigma_n^+}{\mathrm{d}\phi}(\phi_c) > 0. \tag{2.23}$$

The proof of (iii) and (iv) requires knowledge of the neutral curve and this is what we now discuss.

2.2. The neutral curve and stability

We can most easily find the conditions required for local temporal stability of the steady-state S by constructing *the neutral curve*. This is defined in the first quadrant of the (k_n, ϕ)-plane as the locus of those points for which $\mathrm{Re}\{\omega_n^1\} (= \mathrm{Re}\{\omega_n^3\} = \sigma_n^+) = 0$ and is the curve which divides the quadrant into regions corresponding to exponential growth (or decay) of the modes $a_n(t), b_n(t), c_n(t), d_n(t)$, $(n = 0, 1, \ldots)$. On using either (2.13)–(2.14) or (2.17)–(2.18), together with (i), (ii) above, we substitute for $\omega_n = i\eta_n^j, j \in \{-, +\}$ and find the following form for the equation of the neutral curve

$$\phi_c^2(k_n) = \begin{cases} \dfrac{\lambda(k_n^2 + \mu^2 - 1)^2(1 + k_n^2)}{k_n^2(1 - k_n^2)}, & \mu > 1, \\ \dfrac{\lambda k_n^2(1 + k_n^2)}{1 - k_n^2}, & \mu = 1. \end{cases} \tag{2.24}$$

As can be seen from expression (2.24), the neutral curve has a vertical asymptote at $k_n = 1$ and, for $\mu > 1$, a vertical asymptote also at $k_n = 0$. In both cases it exists only for $0 < k_n < 1$. Graphs of the neutral curve for representative values of μ are given in Figures 1(a) and 1(b), corresponding to the differing cases $\mu > 1$ and $\mu = 1$. The neutral curves have a qualitatively similar convex shape for all $\mu > 1$. For $\mu = 1$ the neutral curve is monotonically increasing.

We can establish that the neutral curve is convex for all $\mu > 1$ with an unique minimum in (0, 1). To do so we work with the function

$$f(y) = \frac{(y + \mu^2 - 1)^2(1 + y)}{y(1 - y)} \tag{2.25}$$

on $0 < y < 1$, where we have put $y = k_n^2$. From (2.25) it is straightforward to show that

$$f''(y) = \frac{(\mu^4 + 2\mu^2 - 1)y^3 + 3(\mu^2 - 1)^2\, y^2 - 3(\mu^2 - 1)^2\, y + (\mu^2 - 1)^2}{y^3(1 - y)^3}. \tag{2.26}$$

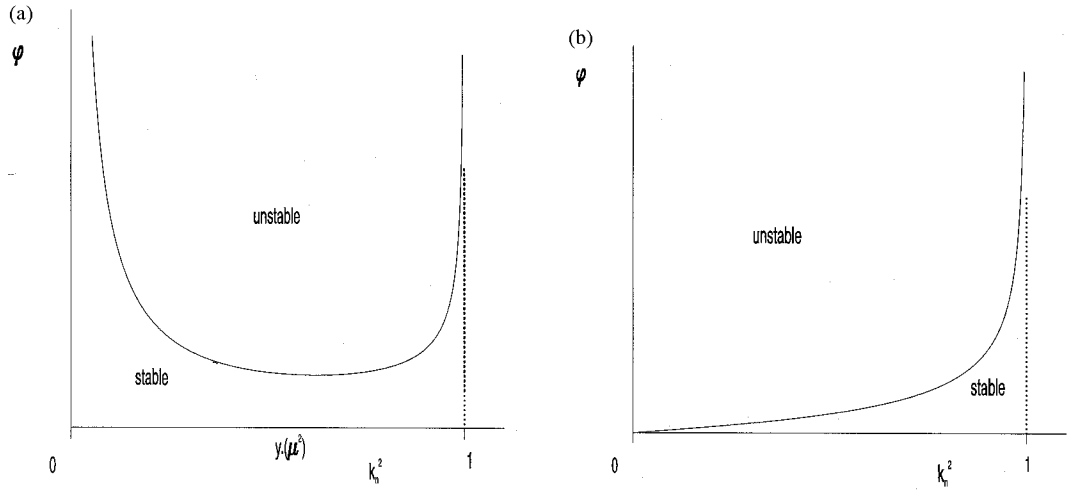

Figure 1. Neutral curves (2.24) for the two cases: (a) $\mu > 1$ (here plotted for $\mu = 2$); (b) $\mu = 1$.

The numerator in expression (2.26) is positive for all $0 < y < 1, \mu \geqslant 1$ hence $f'' > 0$ on (0, 1). This establishes that f is convex on (0, 1), implying that ϕ_c is as well.

To obtain the minimum value of ϕ in (2.24) we notice that putting $f'(y) = 0$ is equivalent to solving

$$-y^3 + (\mu^2 + 1)y^2 + (2\mu^2 - 1)y - (\mu^2 - 1) = 0. \tag{2.27}$$

We can obtain the value of that unique $y_* = y_*(\mu^2)$ in (0, 1) which satisfies (2.27) by using Cardano's formula. When we substitute for this value in f (and so for ϕ), the expression obtained is of little use in practice. However, we can give some results which describe the behaviour of $y_*(\mu^2)$

$$\text{(i)} \quad y_*(\mu^2) < \sqrt{2} - 1. \tag{2.28}$$

To see this we express Equation (2.27) in the form

$$\mu^2 = \frac{(1 - y_*)(1 + y_*^2)}{1 - 2y_* - y_*^2} \equiv h(y_*). \tag{2.29}$$

Then for this to be positive (with $y_* < 1$) we must have the denominator positive and the result follows.

$$\text{(ii)} \quad y_* = 0 \quad \text{when } \mu = 1. \tag{2.30}$$

$$\text{(iii)} \quad y_* \text{ increases monotonically with } \mu. \tag{2.31}$$

To show this, we consider the function $h(y_*)$ defined by Equation (2.29) on $0 \leqslant y_* < \sqrt{2} - 1$. Then

$$h'(y_*) = \frac{(y_*)^4 + 4(y_*)^3 - 6(y_*)^2 + 4y_* + 1}{((y_*)^2 + 2y_* - 1)^2} > 0$$

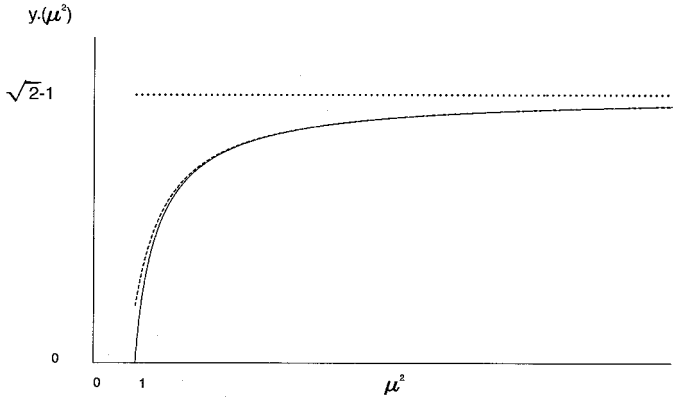

Figure 2. A graph of $y_*(\mu^2)$, the abscissa of the unique minimum on the neutral curve given by (2.24) for $\mu > 1$. Asymptotic expression (2.33) is shown by the broken line.

on its domain, with a vertical asymptote at $y_* = \sqrt{2} - 1$, and the result follows.

It is also straightforward, using standard perturbations methods, to show that

$$y_*(\mu^2) = (\mu^2 - 1) - 4(\mu^2 - 1)^2 + 24(\mu^2 - 1)^3 + \cdots, \quad \text{as } \mu \to 1^+, \tag{2.32}$$

$$y_*(\mu^2) = \sqrt{2} - 1 + \frac{4 - 3\sqrt{2}}{\mu^2} + \frac{31 - 22\sqrt{2}}{\sqrt{2}\mu^4} + \cdots, \quad \text{as } \mu \to \infty. \tag{2.33}$$

In Figure 2 we plot a graph of $y_*(\mu^2)$ against μ^2 which shows the monotone behaviour and the horizontal asymptote at $\sqrt{2} - 1$ as $\mu^2 \to \infty$; the broken line shows the asymptotic expression (2.33). To complete the description of the neutral curve we notice that a special case occurs when $\mu = 1$. As μ decreases to 1, expression (2.32) shows that the vertex (minimum) of the neutral curve gets closer to zero, while still preserving the convex shape. When $\mu = 1$, the curve now connects the point (0, 0) monotonically to the point at infinity along the vertical asymptote at $k_n = 1$.

This discussion gives a clear picture of the form of the neutral curve for all values of $\mu \geqslant 1$. Any point below the neutral curve has $\mathrm{Re}\{\omega_n^i\} < 0, i = 1, 3$, (corresponding to a stable uniform state), while any point above it has at least one eigenvalue with $\mathrm{Re}\{\omega_n^i\} > 0$ leading to (linear) instability.

For given values of μ and λ let M be the unique integer such that

$$4\pi^2 M^2 \lambda \leqslant y_*(\mu^2) \leqslant 4\pi^2 (M+1)^2 \lambda. \tag{2.34}$$

Since the stability of the steady-state S requires $\mathrm{Re}\{\omega_n^i(k_n, \mu, \lambda)\} = \sigma_n^+(k_n, \mu, \lambda) < 0$ for each $i = 1, 3$ and for each $n = 0, 1, 2, \ldots$, it is clear from (2.24), (2.34) and the above discussion that the necessary and sufficient condition for the local temporal stability of S is provided by

$$\phi < \phi_c^M(\mu, \lambda) = \min\{\overline{\phi}_1, \overline{\phi}_2\}, \tag{2.35}$$

where

$$\overline{\phi}_1^2 = \begin{cases} \dfrac{\lambda(4\pi^2 M^2 \lambda + \mu^2 - 1)^2 (1 + 4\pi^2 M^2 \lambda)}{4\pi^2 M^2 \lambda (1 - 4\pi^2 M^2 \lambda)}, & M \neq 0, \\ 0, & \text{otherwise}, \end{cases} \tag{2.36}$$

$$\overline{\phi}_2^2 = \begin{cases} \dfrac{\lambda(4\pi^2(M+1)^2\lambda + \mu^2 - 1)^2(1 + 4\pi^2(M+1)^2\lambda)}{4\pi^2(M+1)^2\lambda(1 - 4\pi^2(M+1)^2\lambda)}, & M < \dfrac{1}{2\pi\sqrt{\lambda}} - 1, \\ 0, & \text{otherwise}, \end{cases} \tag{2.37}$$

with M given from (2.34).

We conclude that, for each $\phi < \phi_c^M$, every term in (2.7)–(2.8) decays exponentially as $t \to \infty$ and any small disturbance imposed upon S will die away. However, if $\phi > \phi_c^M$, there are terms in (2.7)–(2.8) which grow exponentially as $t \to \infty$ and the system will diverge from the spatially uniform stationary state S when perturbed. Thus we restrict attention to the case where $\phi > \phi_c^M(\mu, \lambda)$.

We are now in a position to consider the possibility of nontrivial pattern formation in our system, i.e. to take account of circumstances under which a small amplitude-disturbance to the stationary state S will evolve into a small, but finite amplitude, spatially and/or temporally stable periodic state. As we will see later, any such bifurcation will produce a spatio-temporal symmetry-breaking, leading to the appearance of a both spatially non-homogeneous and temporally periodic pattern in the form of a periodic travelling wave.

2.3. LOCAL BIFURCATION THEORY

We first establish that the neutral curve corresponds to Hopf bifurcations, *i.e.* for each fixed $n = 0, 1, \ldots$, the system undergoes a Hopf bifurcation at $\phi = \phi_c(k_n)$, given by (2.24), where $\sigma_n^+ = 0$ $(= \mathrm{Re}\{\omega_n^i\}, i = 1, 3)$. In doing so we will also complete the proof of the properties (iii), (iv) of the eigenvalues given by (2.22), (2.23). It is straightforward to show that, when $\sigma_n^+ = 0$

$$-\eta_n^- = \mathrm{Im}\{\omega_n^i\} = \tfrac{1}{2}(\gamma_n + \sqrt{\gamma_n^2 + 4q_n}) > 0, \qquad i = 1, 3. \tag{2.38}$$

It is again easy to see (from (2.17)) that $\phi < \phi_c$ $(\phi > \phi_c)$ if and only if $\sigma_n^+(\phi) < \sigma_n^+(\phi_c)$ (respectively $\sigma_n^+(\phi) > \sigma_n^+(\phi_c)$) which proves the uniqueness of ϕ_c. We also need to establish the transversality condition

$$\frac{\mathrm{d}\sigma_n^+}{\mathrm{d}\phi}(\phi_c) > 0. \tag{2.39}$$

To do so, we start by noting that

$$\lim_{\gamma_n \to \infty} \sigma_n^+(\gamma_n) = 1 - k_n^2 > 0. \tag{2.40}$$

We then assume the contrary, *i.e.* that $\mathrm{d}\sigma_n^+/\mathrm{d}\phi(\phi_c) \leqslant 0$. This implies that σ_n^+ is locally decreasing around $\phi = \phi_c$. Consequently there is a number ϕ^1 such that $\phi_c < \phi^1$ and: $0 = \sigma_n^+(\phi_c) \geqslant \sigma(\phi^1)$. But $\sigma_n^+(\phi^1) \neq 0$, because there is a unique ϕ_c for given k_n and given values of the other parameters. Thus $\sigma_n^+(\phi^1) < 0$. However $\lim_{\phi\to\infty} \sigma_n^+(\phi) > 0$ from (2.40). Thus there must be a $\phi^2 > \phi^1$ such that $\sigma_n^+(\phi^2) = 0$, which is a contradiction.

The conditions for a Hopf bifurcation at $\phi = \phi_c(k_n)$ are satisfied (see, for example, [18, Chapter 11]) and a unique limit cycle with amplitude of $O(|\phi - \phi_c|^{1/2})$ for $|\phi - \phi_c| \ll 1$ is born as the neutral curve is crossed. The stability of this limit cycle needs further consideration and will be addressed below when we consider a weakly-nonlinear analysis.

The oscillatory behaviour of the Fourier coefficients in (2.7)–(2.8) (or the purely imaginary nature of an ω_n^i $(i = 1, 2, 3, 4)$ in expressions (2.15)) corresponds to travelling waves in the original reaction-diffusion-convection system. Thus this DIFICI instability gives rise to spatio-temporal structures in the form of travelling waves at the primary bifurcation from the spatially uniform stationary state S.

Further information about these bifurcation points can be given at this stage. By definition the first bifurcation occurs at $\phi = \phi_c^M$ when $k_n = k_n^M$ corresponding to the integer (see (2.35)–(2.37))

$$n^M = \begin{cases} 0, & \overline{\phi}_1, \overline{\phi}_2 = 0, \\ M, & \overline{\phi}_1 < \overline{\phi}_2, \\ M+1, & \overline{\phi}_1 > \overline{\phi}_2. \end{cases} \tag{2.41}$$

We have

$$n^M = 0, \quad \text{if } \lambda \geqslant \frac{1}{4\pi^2}, \tag{2.42}$$

$$n^M = 1, \quad \text{if } \frac{1}{16\pi^2} < \lambda < \frac{1}{4\pi^2}, \tag{2.43}$$

$$n^M = 2, \quad \text{if } \frac{1}{36\pi^2} < \lambda < \frac{1}{16\pi^2}, \tag{2.44}$$

(for (2.44) see Section 3, relation (3.29)) and so on.

We can also give information about the number of local bifurcations occurring in $\phi \geqslant \phi_c^M$. From (2.24), (2.37), (2.42) we have that, if $\lambda \geqslant 1/4\pi^2$, then the only local bifurcation point in $\phi > \phi_c^M$ is that at $\phi = \phi_c^M = 0$ which corresponds to $\mu = 1, k_n^M = 0$. This leads to a spatially homogeneous, temporally periodic solution which is stable when $0 < 1 - \mu \ll 1$. This corresponds to the limit cycle of the well-stirred system and we would expect only homogeneous (trivial) pattern formation in our system for $\phi > 0$ as no further local bifurcation can appear in this range. For $\mu > 1$ (and $\phi = 0$) the steady-state S remains locally and absolutely stable. However, for $\lambda < 1/4\pi^2$, the total number of local bifurcations in $\phi \geqslant \phi_c^M$ is N, where N is the unique integer defined by

$$\frac{1}{2\pi\sqrt{\lambda}} - 1 \leqslant N < \frac{1}{2\pi\sqrt{\lambda}}. \tag{2.45}$$

Thus, the linearized theory has enabled us to identify the bifurcations points in $\phi > \phi_c^M$. The nature of the bifurcation and the spatially non-uniform structures to which the system could evolve when the stationary state S is unstable can be determined only by a consideration of the full nonlinear problem. To treat this aspect we start by deriving a weakly-nonlinear analysis valid close to ϕ_c and extend this by numerical solutions of Equations (1.7)–(1.9).

3. Weakly-nonlinear analysis

We start by considering the solution near the Hopf bifurcation points identified above to see how the small linear growth rate for conditions close to neutral stability can be balanced by the

weak nonlinear decay to produce equilibrated patterns at small amplitude. We have seen in the previous section that, in order for the system to bifurcate locally to a stable non-homogeneous, temporally periodic (flow-generated) pattern, we must have $\mu > 1$ and $\phi_c^M > 0$. This, in turn, gives a necessary condition for the local bifurcation to stable pattern forms that

$$4\pi^2\lambda < 1, \qquad \mu > 1. \tag{3.1}$$

We will now suppose that μ, λ satisfy these conditions. In this case each bifurcating solution with a wave number $k_n = 2n\pi\sqrt{\lambda}, (n = 1, 2, \ldots)$ corresponds to a bifurcation value of the parameter

$$\phi_n^2(k_n) = \frac{\lambda(k_n^2 + \mu^2 - 1)^2(1 + k_n^2)}{k_n^2(1 - k_n^2)}. \tag{3.2}$$

For (3.2) we require that $k_n^2 = 4\pi^2 n^2\lambda < 1$. We now consider values of ϕ such that $0 < |\phi - \phi_n| \ll 1$ and construct an approximation for the new bifurcated pattern valid at least for ϕ in this weak nonlinear limit. Also in this case we will consider that the pattern is obtained by evolution from initial conditions with only the wave number k_n present.

The method we use is similar to that described in [15] and [16]. We begin by putting

$$\phi = \phi_n + \varepsilon^2\rho, \qquad 0 < \varepsilon \ll 1, \tag{3.3}$$

with ϕ_n given by (3.2) and where $\rho \in \{-1, 1\}$. Specifically $\rho = 1$ when the new pattern bifurcates initially into $\phi > \phi_n$ or $\rho = -1$ when the new pattern bifurcates initially into $\phi < \phi_n$. The next step is to expand the solution about the stationary state S in powers of ε. At $O(\varepsilon^3)$ we find that the cubic nonlinearity reproduces the fundamental neutral mode as an inhomogeneous forcing term rendering the expansion non-uniform when t is of $O(\varepsilon^{-2})$. We remove this difficulty by using the method of multiple scales [19, Sect. 3.6], where we allow our solution to depend on the slow time $\tau = \varepsilon^2 t$. This has the effect of removing the secular terms which arise at $O(\varepsilon^3)$. Thus we start by putting

$$\begin{cases} a(x, t, \tau) = \dfrac{1}{\mu} + a_1\varepsilon + a_2\varepsilon^2 + a_3\varepsilon^3 + \cdots, \\ b(x, t, \tau) = \mu + b_1\varepsilon + b_2\varepsilon^2 + b_3\varepsilon^3 + \cdots, \end{cases} \tag{3.4}$$

where the coefficients a_i, b_i, are all functions of x and the two time variables t and τ.

We introduce the linear matrix differential operator

$$L = L_c = \begin{pmatrix} \dfrac{\partial}{\partial t} + \mu^2 & 2 \\ -\mu^2 & \dfrac{\partial}{\partial t} - \lambda\dfrac{\partial^2}{\partial x^2} + \phi_n\dfrac{\partial}{\partial x} - 1 \end{pmatrix}. \tag{3.5}$$

Also we recall that $\omega_n^c = \omega_n(\phi_n) = -i\eta_n^-$ with $-\eta_n^- > 0$ (see (2.18)). In the sequel we shall denote (for convenience) $-\eta_n^- = \eta_n > 0$. The leading-order terms satisfy the linear homogeneous problem (2.3)–(2.6) with ϕ replaced by ϕ_n. That is

$$L_c \begin{pmatrix} a_1 \\ b_1 \end{pmatrix} = \begin{pmatrix} 0 \\ 0 \end{pmatrix}. \tag{3.6}$$

The solution of these equations can be written in terms of Fourier series with all wave numbers present. However, with ϕ close to ϕ_n and for initial conditions which contain only the particular wave number k_n (with ϕ_n given by (3.2)), there is only a neutral mode. Consequently our solution will approach this mode in the limit as $t \to \infty$ and from (2.15) we find

$$\begin{pmatrix} a_1 \\ b_1 \end{pmatrix} = \begin{pmatrix} A_1 \exp(i\eta_n t) + A_2 \exp(-i\eta_n t) \\ C_1 \exp(i\eta_n t) + C_2 \exp(-i\eta_n t) \end{pmatrix} \cos(kx) + \begin{pmatrix} B_1 \exp(i\eta_n t) + B_2 \exp(-i\eta_n t) \\ D_1 \exp(i\eta_n t) + D_2 \exp(-i\eta_n t) \end{pmatrix} \sin(kx),$$

with $k = k(n) = 2n\pi$. Here $A_i, B_i, C_i, D_i, (i = 1, 2)$ are the Fourier coefficients which are mentioned in (2.15) and from the linear algebraic system we find that they satisfy

$$\frac{A_1}{C_1} = \frac{B_1}{D_1} = \frac{-2}{\mu^2 + i\eta_n}, \qquad \frac{A_2}{C_2} = \frac{B_2}{D_2} = \frac{-2}{\mu^2 - i\eta_n}, \qquad \frac{D_1}{C_1} = -i, \qquad \frac{D_2}{C_2} = i. \tag{3.7}$$

Thus we have the solution to (3.6) in the form

$$\begin{pmatrix} a_1 \\ b_1 \end{pmatrix} = A(\tau) \exp(i(\eta_n t - kx)) \begin{pmatrix} d_1 \\ d_2 \end{pmatrix} + \overline{A}(\tau) \exp(-i(\eta_n t - kx)) \begin{pmatrix} \overline{d_1} \\ \overline{d_2} \end{pmatrix}, \tag{3.8}$$

with $d_1/d_2 = -2/(\mu^2 + i\eta_n)$ and where A is, at this stage, an undetermined amplitude.

At $O(\varepsilon^2)$ we have the linear inhomogeneous problem (the difference with the previous stage being that we now have quadratic forcing terms on the right-hand side resulting from the nonlinear interaction of the leading-order terms)

$$L_c \begin{pmatrix} a_2 \\ b_2 \end{pmatrix} = \begin{pmatrix} -1 \\ 1 \end{pmatrix} \left(2\mu a_1 b_1 + \frac{b_1^2}{\mu} \right). \tag{3.9}$$

After some algebra we find that the solution of this problem, in the limit as $t \to \infty$, is

$$\begin{pmatrix} a_2 \\ b_2 \end{pmatrix} = \frac{|A|^2 E}{\mu^2} \begin{pmatrix} -1 \\ 0 \end{pmatrix} + \frac{A^2 F}{\Delta} \begin{pmatrix} -(4k_n^2 + 1 + 2i(\eta_n - \gamma_n)) \\ 2i\eta_n \end{pmatrix} \times \exp(2i(\eta_n t - kx)) + c.c. + B \begin{pmatrix} a_1 \\ b_1 \end{pmatrix} \tag{3.10}$$

where B is a further function of the slow time τ and where

$$F = 2\mu d_1 d_2 + \frac{d_2^2}{\mu}, \qquad E = 2\mu(\overline{d_1} d_2 + d_1 \overline{d_2}) + \frac{2|d_2|^2}{\mu}, \tag{3.11.1}$$

$$\Delta = (4k_n^2 + 1)\mu^2 - 4\eta_n(\eta_n - \gamma_n) + 2i[\eta_n(4k_n^2 + \mu^2 - 1) - \gamma_n \mu^2]. \tag{3.11.2}$$

At $O(\varepsilon^3)$ we find again a linear inhomogeneous problem, but now the right side contains forcing terms arising from the nonlinear interaction of the previous terms in the expansion

$$L_c \begin{pmatrix} a_3 \\ b_3 \end{pmatrix} = \frac{-\partial}{\partial \tau} \begin{pmatrix} a_1 \\ b_1 \end{pmatrix} - \alpha \begin{pmatrix} 0 & 0 \\ 0 & 1 \end{pmatrix} \begin{pmatrix} \nabla a_1 \\ \nabla b_1 \end{pmatrix} + \begin{pmatrix} -1 \\ 1 \end{pmatrix} \times \left(2\mu(a_1 b_2 + a_2 b_1) + \frac{2}{\mu} b_1 b_2 + a_1 b_1^2 \right). \tag{3.12}$$

At this stage it can be seen that, when analysing the nature of the solution to this equation at $t \to \infty$, we find resonant terms. They can have various possible sources, but our method allows us to remove them and, following the method of multiple scales, we equate these terms with zero. This leads to an equation for the complex amplitude $A(\tau)$ which is the Stuart–Landau amplitude equation associated with the corresponding DIFICI bifurcation. In fact this is equivalent to applying the solvability criterion for the linear operator L_c.

This complex amplitude is most conveniently expressed as

$$A(\tau) = R(\tau)\exp(i\theta(\tau)), \tag{3.13}$$

where $R \geqslant 0$ and θ are the real, slowly-varying amplitude and phase. We obtain, after a long but straightforward calculation, that

$$\frac{\mathrm{d}R}{\mathrm{d}\tau} = CR(\alpha_1 R^2 + \beta_1 \rho), \tag{3.14}$$

where C is a constant, positive for all values of the parameters, given by

$$C^{-1} = \frac{4\mu^4(\mu^4 + 2\mu^2(k_n^2 - k_n^4) + (k_n^2 - 1)^2)}{(1 - k_n^2)^2},$$

and where

$$\alpha_1 = \frac{8}{3}\mu^8 \frac{(1 + k_n^2)(P_2(k_n^2) + \mu^2 P_3(k_n^2))}{(1 - k_n^2)^3(1 - k_n^2 + 4k_n^4 + 4k_n^6)}, \tag{3.15}$$

where

$$P_2(k_n^2) = 36k_n^{10} - 32k_n^8 + 3k_n^6 - 18k_n^4 + 15k_n^2 - 4, \tag{3.16}$$

$$P_3(k_n^2) = 24k_n^8 - 76k_n^6 + 18k_n^4 - 7k_n^2 + 1, \tag{3.17}$$

$$\beta_1 = (8n\pi)\mu^6 \sqrt{\frac{1 + k_n^2}{1 - k_n^2}} > 0. \tag{3.18}$$

Reusing, for simplicity, the notation $y = k_n^2, 0 < y < 1$, we note that

$$P_2 = (y - 1)(36y^4 + 4y^3 + 7y^2 - 11y + 4),$$
$$P_3 = (6y - 1)(4y^3 - 12y^2 + y - 1).$$

Consider Equation (3.14) with an initial condition $R(0) = R_0 > 0$. If $\alpha_1 < 0$, we take $\rho = 1$, so that the bifurcated pattern form starts, initially at least, in $\phi > \phi_n$. From (3.14) we find that

$$R^2(\tau) = \frac{R_0^2 \beta_1}{(\beta_1 + \alpha_1 R_0^2)\exp(-2\beta_1 \tau) - \alpha_1 R_0^2}, \tag{3.19}$$

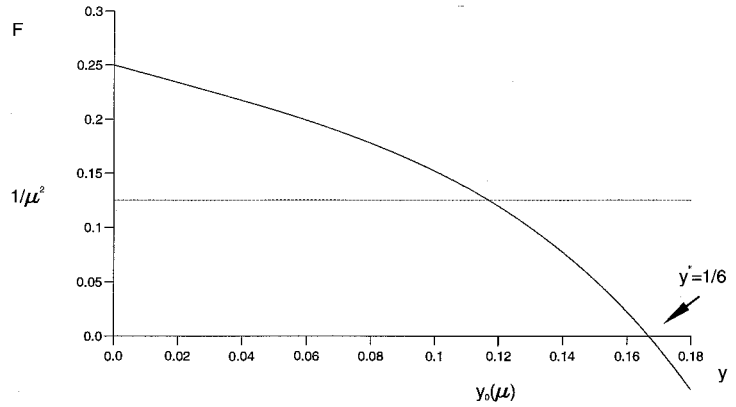

Figure 3. A graph of $F(y) = P_3(y)/(-P_2(y))$, where $P_2(y)$ and $P_3(y)$ are defined from (3.16–3.17). $y^* = \frac{1}{6}$ is the only zero of $P_3(y)$ on $(0, 1)$. The broken line indicates the values of μ^{-2} at which $\alpha_1 = 0$.

and we deduce that the nontrivial steady-state of Equation (3.14), which corresponds to an oscillatory solution in the original problem

$$R_s = \sqrt{\frac{\beta_1}{|\alpha_1|}} \tag{3.20}$$

is stable. However, if $\alpha_1 > 0$, we take $\rho = -1$ and the bifurcated pattern appears initially in $\phi < \phi_n$. A further consideration of Equation (3.14) shows that, in this case, the solution is

$$R^2(\tau) = \frac{R_0^2 \beta_1}{\alpha_1 R_0^2 - (\alpha_1 R_0^2 - \beta_1)\exp(2\beta_1 \tau)} \to 0 \quad \text{as } \tau \to \infty$$

and the nontrivial steady state $R_s = \sqrt{\beta_1/\alpha_1}$ is unstable with the trivial steady state, $R_s = 0$, now being stable.

This leads us to consider the function $\alpha_1 = \alpha_1\ (y)$ for $0 < y < 1$. It is clear that its denominator is positive. We also find that $P_2 < 0$ for all y in $(0, 1)$ and that $P_3 = 0$ has only one solution $y = y^* = \frac{1}{6}$ in $(0, 1)$ with $P_3 > 0$ for $y < y^*$. For given $\mu > 1$ it is easy to see that $g(y) = P_2(y) + \mu^2 P_3(y) \leqslant 0$ if $1 < \mu \leqslant 2$ and for $\mu > 2$ there is an unique $y = y_0(\mu)$ in $(0, y^*)$ such that $g(y) = 0$. To see this, we have plotted the graph of the function $F(y) = P_3(y)/(-P_2(y))$ in Figure 3 from which we observe that $\alpha_1 = 0$ if and only if $F(y) = 1/\mu^{-2}$. This clearly has an unique solution $y = y_0\ (\mu)$ for given $\mu > 2$ (a typical example is illustrated in Figure 3). We conclude that

$$\alpha_1 < 0 \quad \text{if } 1 < \mu \leqslant 2 \quad \text{and also if } \mu > 2 \quad \text{for } y_0(\mu) < y < 1,$$

and

$$\alpha_1 > 0 \quad \text{if } \mu > 2 \quad \text{for } 0 < y < y_0(\mu). \tag{3.21}$$

The phase equation is found in a similar manner as

$$\frac{\mathrm{d}\theta}{\mathrm{d}\tau} = \alpha_2 R^2 + \beta_2, \tag{3.22}$$

with R given by Equation (3.14) and where

$$\alpha_2(y) = -\frac{8}{3}C\mu^8 \frac{P_4(y) + \mu^2 P_5(y)}{(1-y)^2(1-y+4y^2+4y^3)}\sqrt{\frac{1+y}{1-y}}, \tag{3.23}$$

with

$$P_4(y) = 36y^5 + 28y^4 - 69y^3 + 7y^2 - 3y + 1,$$
$$P_5(y) = -24y^4 + 16y^3 - 6y^2 - 6y + 4$$

and

$$\beta_2(y) = C(8n\pi)\mu^6 \frac{(\mu^2 + y - y^2)}{(1-y)^2}. \tag{3.24}$$

Equation (3.22) can be integrated once R is known from Equation (3.14).

This discussion leads to the following conclusions for pattern formation as the parameters ϕ, μ, λ of our system are varied (we will denote by $\phi_{n,i}$ the value of ϕ at the bifurcation value with wave number k_i). Take first the case when only the first mode $(n = 1)$ has linear growth with the uniform state being stable to all other modes $(n = 2, 3, \ldots)$. This requires the condition

$$\tfrac{1}{4} < 4\pi^2\lambda < 1. \tag{3.25}$$

Hence in this case $y > \frac{1}{4} > y^*$ and the bifurcation is always supercritical (stable). From (3.8), (3.13) we find the form of the solution branches for a and b to be as follows

$$\begin{aligned} a(x,t,\varepsilon) &= \mu^{-1} + 4R(\tau)\cos(\eta_n t - kx + \theta(\tau))(\phi - \phi_n)^{1/2} + \cdots, \\ b(x,t,\varepsilon) &= \mu + 2\sqrt{\eta_n^2 + \mu^4}R(\tau)\cos(\eta_n^+ t - kx + \theta(\tau))(\phi - \phi_n)^{1/2} + \cdots. \end{aligned} \tag{3.26}$$

In the limit of $t \to \infty$ equilibrated pattern forms are obtained from (3.26) if we replace $R(\tau)$ with R_s (given from (3.20)) and $\theta(\tau)$ with $\theta_s^n\tau + \theta_0$ (θ_0 is an arbitrary constant) where: $\theta_s^n = \alpha_2 R_s^2 + \beta_2$. These solutions are periodic travelling-wave solutions of our system with

$$\begin{aligned} &\text{amplitude } A_s^n = 2R_s(\phi - \phi_n)^{1/2} + \cdots, \\ &\text{period } T_s^n = \frac{2\pi}{\eta_n + \theta_s^n(\phi - \phi_n) + \cdots}. \end{aligned} \tag{3.27}$$

Both solutions are dependent on an arbitrary phase θ_0 (this is to be expected, as our system is invariant to the change of co-ordinates: $x \to x + \rho$ mod(1)). From (3.27) we have that A_s^n is of $O(|\phi - \phi_n|^{1/2})$, while the correction to the period is $O(|\phi - \phi_n|)$ as $\phi \to \phi_n$. A graph of the amplitude R_s (as given by (3.20)) with respect to the first wave number $(k_1 = 2\pi\sqrt{\lambda}, 1/16\pi^2 < \lambda < 1/4\pi^2)$ is shown in Figure 4.

Next consider the case when the dimensionless parameters are such that the first two modes can grow $(n = 1, n = 2)$ with all the other modes remaining stable. This requires the condition

$$\tfrac{1}{9} < 4\pi^2\lambda < \tfrac{1}{4}. \tag{3.28}$$

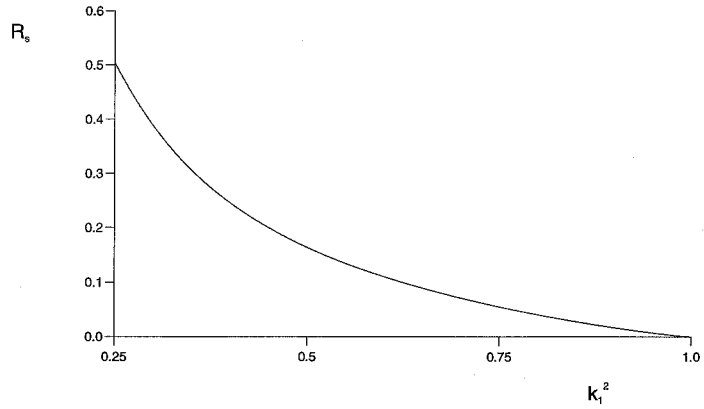

Figure 4. A graph of R_s as given by (3.20), against the first wave number k_1.

Now for given $\mu > 1$, $y = 4\pi^2\lambda$ can lie in one of the ranges: $\frac{1}{9} < y < y_0(\mu)$, $y_0(\mu) < y < \frac{1}{4}$. We will show now that in either case the primary bifurcation from the stationary state S is always supercritical (stable). In fact from (3.20)–(3.21) this needs to be proved only in the case when $\mu > 2$ and $\frac{1}{9} < y < y_0(\mu)$. Also in this case we have $k_2^2 = 4y > \frac{4}{9} > \frac{1}{4}$, so that the only possible subcritical bifurcation arises at $\phi = \phi_{n,1}$. However, we have the inequality

$$\phi_{n,1} > \phi_{n,2}. \tag{3.29}$$

To establish this result we require to show, on using expression (2.24) for $\phi_{n,1}$ and $\phi_{n,2}$ that

$$\left(\frac{\mu^2 + y - 1}{\mu^2 + 4y - 1}\right)^2 > \frac{(1+4y)(1-y)}{4(1-4y)(1+y)}, \tag{3.30}$$

for $\frac{1}{9} < y < \frac{1}{6}$. Consider

$$G(y) = \sqrt{\frac{(1+4y)(1-y)}{4(1-4y)(1+y)}},$$

(clearly $G(y) < 1$ on $0 < y < y^* = \frac{1}{6}$). Then (3.30) can be written as

$$\mu^{-2} < H(y) \quad \text{for } \tfrac{1}{9} < y < y_0(\mu), \tag{3.31}$$

where

$$H(y) = \frac{1 - G(y)}{(4y-1)G(y) + 1 - y}.$$

We find that H is strictly decreasing, so that $H(y) > H(y_0(\mu))$ for $y < y_0(\mu)$. From (3.21) it only remains to compare $H(y_0(\mu))$ with $F(y_0(\mu))$. A consideration of the difference H-F shows that it is always positive in $(0, y^*)$, which completes the proof of (3.29).

An examination of the above proof shows that it is in fact valid for all $0 < y < y^*$, so that we have in general that $\phi_{n,1} > \phi_{n,2}$. From this we can immediately deduce that the

first bifurcation is also supercritical in the case with three unstable modes (we note that this requires $\frac{1}{16} < y = 4\pi^2\lambda < \frac{1}{9}$, but we have $k_2^2 = 4y > \frac{1}{4} > y^*$ and $k_3^2 = 9y > \frac{9}{16} > y^*$). We are able to extend this result to show that the primary bifurcation is supercritical when $n > 7$. To do so, we note that the first bifurcation corresponds to the integer M as given by (2.34), (2.41). We need to prove the required result only when $\mu \geqslant 2$ and on using property (2.31) for $y_*(\mu^2)$, we have

$$y_M = 4(M+1)^2\pi^2\lambda > y_*(\mu^2) > y_*(4) = 0{\cdot}348\cdots = y_1. \tag{3.32}$$

Now the general condition for unstable modes is

$$\frac{1}{(n+1)^2} < 4\pi^2\lambda < \frac{1}{n^2}. \tag{3.33}$$

Combining (3.32), (3.33) we then have that $M > n\sqrt{y_1} - 1$. In this case we see that $y_{M-1} = 4M^2\pi^2\lambda > \frac{1}{6} = y^*$ provided that $n > 7{\cdot}751$. We are unable to prove this general property of the first bifurcation directly for the remaining cases $n = 4, 5, 6, 7$. However, numerical evidence strongly suggests that it is true in these particular cases as well.

We can now complete this discussion by summarising the general case when any finite number of modes become unstable:

- If $1 < \mu \leqslant 2$ all the bifurcations from the branch of the steady-states S are *supercritical* and thus, at least initially, the new bifurcating solutions are partially stable. This means that these patterns are temporally stable to perturbations composed of all except a finite set of wave numbers k_n. In fact this set of wave numbers, to which the bifurcating patterns are unstable, is included in the set of wave numbers associated with bifurcations at values smaller than or equal to ϕ.
- If $\mu > 2$ the primary bifurcation still remains *supercritical*, while the secondary, tertiary, etc., bifurcations from the branch of the stationary states S will produce partially stable solutions which are locally *subcritical* if they start at $\phi = \phi_{n,i}$ with the corresponding wave number k_n^i such that $\alpha_1(y) = \alpha_1((k_n^i)^2) > 0$ and *supercritical* otherwise.

4. Numerical results

4.1. Numerical method

We use a combination of two numerical procedures which enables us to check the analytical results of the previous sections and also to extend the bifurcating patterns well away from the bifurcation points. The first procedure used was the spectral decomposition together with the numerical continuation package PATH [20]. This procedure has several major advantages in that it

(i) finds very accurately the primary bifurcating points;
(ii) calculates the temporal eigenvalues at each point and thus the stability of the solution is determined;
(iii) allows us to plot a measure of the solution and to construct the bifurcation diagrams.

The second method was to obtain complete numerical solutions for the full initial-boundary-value problem (1.7–1.9). An implicit Crank–Nicolson discretization method was used in which the derivatives in time were replaced by forward differences and all other terms averaged over

the time step. In these equations space derivatives were replaced by central differences. We solved the resulting sets of nonlinear algebraic equations using the Successive-Over-Relaxation iterative method which was deemed to be convergent if

$$\Delta a^{(s)} = \max\{|a_i^{(s)} - a_i^{(s-1)}|, \qquad i = 1, \ldots, n\} < \varepsilon, \tag{4.1}$$

$$\Delta b^{(s)} = \max\{|b_i^{(s)} - b_i^{(s-1)}|, \qquad i = 1, \ldots, n\} < \varepsilon, \tag{4.2}$$

where: n is the number of the grid points used in the discretization of the interval $(0, 1)$, the notation $(\,)_i$ means the value of the solution at the grid point x_i, the superscript s is the order of iteration and ε is a measure of the accuracy, typically $\varepsilon = 10^{-9}$. This procedure was found to converge quickly, usually taking between five and ten iterations at each time step. Care was taken in order to ensure that the numerical solutions were independent of the mesh size. Values of $n = 100$ (giving $\Delta x = 0{\cdot}01$) and a time step, $\mathrm{d}t = 0{\cdot}0025$, were used for the results which are presented. We present our bifurcation diagrams, using $b(0, t)$ as a measure of the solution and for simplity we present only the upper branches of these solutions. (For non-uniform states there is also a corresponding lower branch, which is qualitatively similar to the upper branch.)

4.2. Numerical results

We illustrate the different cases that were found from our weakly-nonlinear analysis. Take first the case when only the first mode with the wave number k_1 is unstable. Thus we have $\frac{1}{4} < k_1^2 < 1$ and in this case the only possibility is a supercritical primary Hopf bifurcation. To illustrate this case, we took $\lambda = 0{\cdot}01, \mu = 2$, giving $\phi_{n,1} = 0{\cdot}82022$. The bifurcated travelling-wave-solution branch obtained from PATH is given in Figure 5(a). The stable pattern emerged at $\phi_{n,1}$ into $\phi > \phi_{n,1}$ and remained stable for all the ϕ computed (up to $\phi = 75$). We also present a comparison between the analytically and numerically determined values of $b(0, t)$ for ϕ close to $\phi_{n,1}$ in Figure 5(b). The analytical amplitude is obtained from (3.26), (3.27) as

$$A_b = 2\sqrt{\eta_n^2 + \mu^4}R_s(\phi - \phi_{n,1})^{1/2},$$

where here $R_s = 0{\cdot}25073$ and $\eta_n^+ = 6{\cdot}0723$. The two values are in good agreement close to $\phi_{n,1}$ and diverge slowly (as expected) as ϕ is increased. PATH also gives the period for each value of the parameter and this was also found to be in very good agreement with our analytical results (3.27). The travelling waves profiles for a range of values of ϕ for this case are shown in Figures 5(c) (for a) and 5(d) (for b) with these profiles being plotted after a sufficiently long time had passed for any transients to have died out. These figures show that, in each case, a single period travelling wave is produced in which the amplitude of the wave in a decreases as ϕ is increased (by $\phi = 75{\cdot}0$ this wave is almost indistinguishable from S). The concentration b undergoes greater variations and this remains so as ϕ is increased.

Next consider the case when the modes with wave numbers k_1, k_2 become unstable. We have seen that there are three cases to consider, namely when $1 < \mu \leqslant 2$ with all the bifurcations from the steady-state solutions S being supercritical and when $\mu > 2$ with two different cases depending on whether $y_0(\mu) < k_1^2 < \frac{1}{4}$ (with all the bifurcations being supercritical) or $\frac{1}{9} < k_1^2 < y_0(\mu)$, giving $\phi_{n,1} > \phi_{n,2}$, (with the bifurcation at $\phi_{n,1}$ being subcritical). The first case $(1 < \mu \leqslant 2)$ is illustrated in Figure 6 where we took a case when

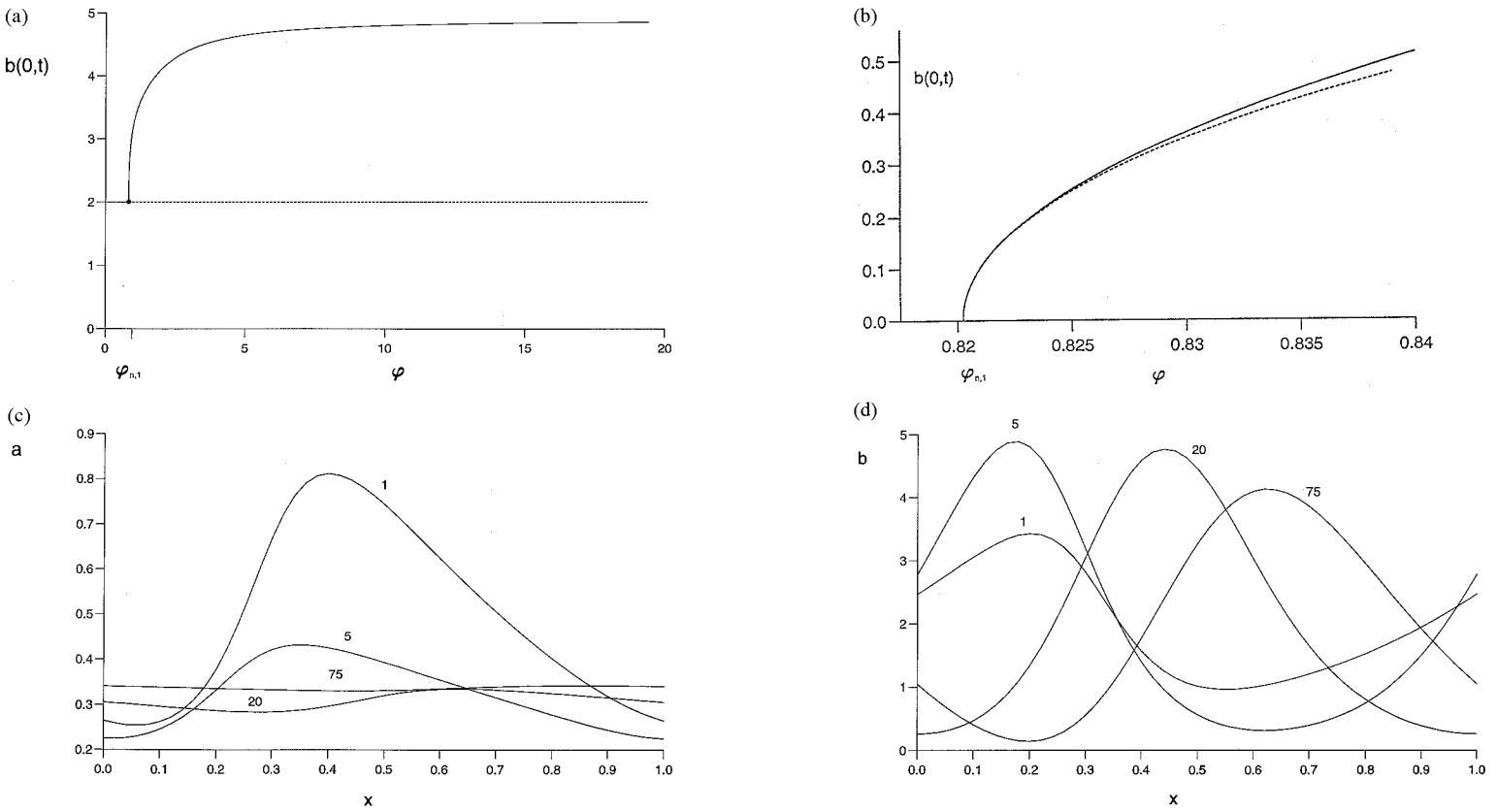

Figure 5. (a) Bifurcation diagram (plot of $b(0,t)$ against ϕ) for $\mu = 2{\cdot}0, \lambda = 0{\cdot}01$, (one wave number unstable), • represent the primary Hopf bifurcation; (b) a comparison between numerical (broken line) and analytical solution (full line); travelling wave profiles; (c) for a; (d) for b, for a range of value of ϕ.

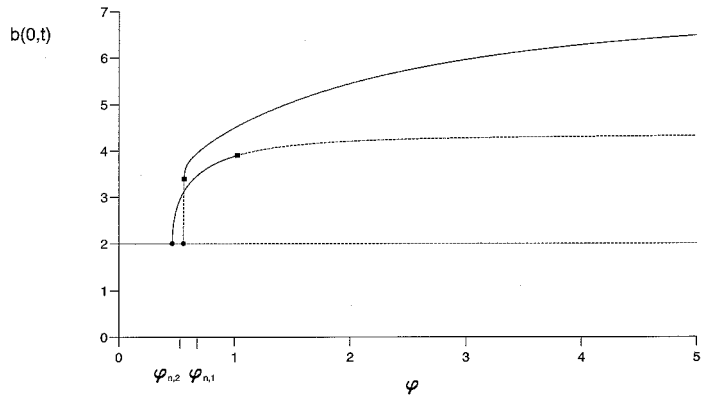

Figure 6. Bifurcation diagram for $\mu = 2{\cdot}0, \lambda = 0{\cdot}003$ (two wave numbers unstable); • represents the primary Hopf bifurcation; ■ represents secondary bifurcations.

$\frac{1}{9} < k_1^2 = 0{\cdot}1184 < y_0$ in order to compare it with the similar case when $\mu > 2$, taking values $\lambda = 0{\cdot}003$ and $\mu = 2$ (giving $\phi_{n,1} = 0{\cdot}559, \phi_{n,2} = 0{\cdot}4625$) being used for this figure. Here the bifurcation diagram is more complicated. The primary bifurcation is at $\phi_{n,2}$ and produces stable patterns in $\phi > \phi_{n,2}$. These lose stability at $\phi = 1{\cdot}05$ at a secondary Hopf bifurcation point and remain unstable as ϕ is increased. The unstable, secondary branch of solutions emerging at $\phi_{n,1}$ into $\phi > \phi_{n,1}$ becomes stable at $\phi = 0{\cdot}565$ at another secondary Hopf point with this branch of solutions remaining stable as ϕ is increased to large values. Thus, we have a parameter region with multiple locally absolutely stable patterns, a situation different to the previous studies of this model in the absence of the flow [15, 16, 17].

Stable travelling waves arising from the primary bifurcations are illustrated in Figures 7(a) and (b) (for $\phi = 0{\cdot}5$). Here we can see a doubly-periodic structure to the pattern form resulting from this primary bifurcation being associated with the wave number k_2. Stable patterns on the secondary solution branch are illustrated in Figures 7(c) and (d) (for $\phi = 2$). These show the single periodic behaviour associated with bifurcations with wave number k_1. The existence of the two stable travelling waves is illustrated in Figures 7(e) and (f) where we plot concentration profiles for $\phi = 0{\cdot}8$. These are both stable, the singly-periodic wave emanating from $\phi_{n,1}$ and the doubly-periodic one from $\phi_{n,2}$. This figure shows that the profiles for the doubly-periodic waves have a sinusoidal form, whereas the singly-periodic waves have a ramp-like form for a and a pulse-like form for b. This becomes more pronounced as ϕ is increased (see Figures 7(g) and (h) where we plot profiles for $\phi = 25{\cdot}0$).

The second possibility is illustrated in Figure 8, where we took $\mu = 3, \lambda = 0{\cdot}0043$ giving $\phi_{n,1} = 1{\cdot}5433, \phi_{n,2} = 1{\cdot}5796$. In this case $k_1^2 = 0{\cdot}1697 > y_0(\mu) = y_0(3) = 0{\cdot}1242$ and both branches start in the supercritical parameter region. This situation is very similar to the case when only the first mode is unstable. Despite starting at very close bifurcation points, the unstable oscillatory solution born at $\phi_{n,2}$ does not interact with the stable pattern arising at $\phi_{n,1}$.

The third possibility is illustrated in Figure 9(a), where we have taken $\mu = 3, \lambda = 0{\cdot}003$ so that $\phi_{n,1} = 1{\cdot}455, \phi_{n,2} = 1{\cdot}128$. Here the picture is very similar to the case illustrated in Figure 6. The main difference is that now the unstable pattern starting at $\phi_{n,1}$ goes initially into $\phi < \phi_{n,1}$ in a very narrow region. This accords with our nonlinear analysis, because in this case we have $\frac{1}{9} < k_1^2 = 0{\cdot}1184 < y_0(\mu) = y(3) = 0{\cdot}1242 < \frac{1}{6}$ (see Figure 9(b) where

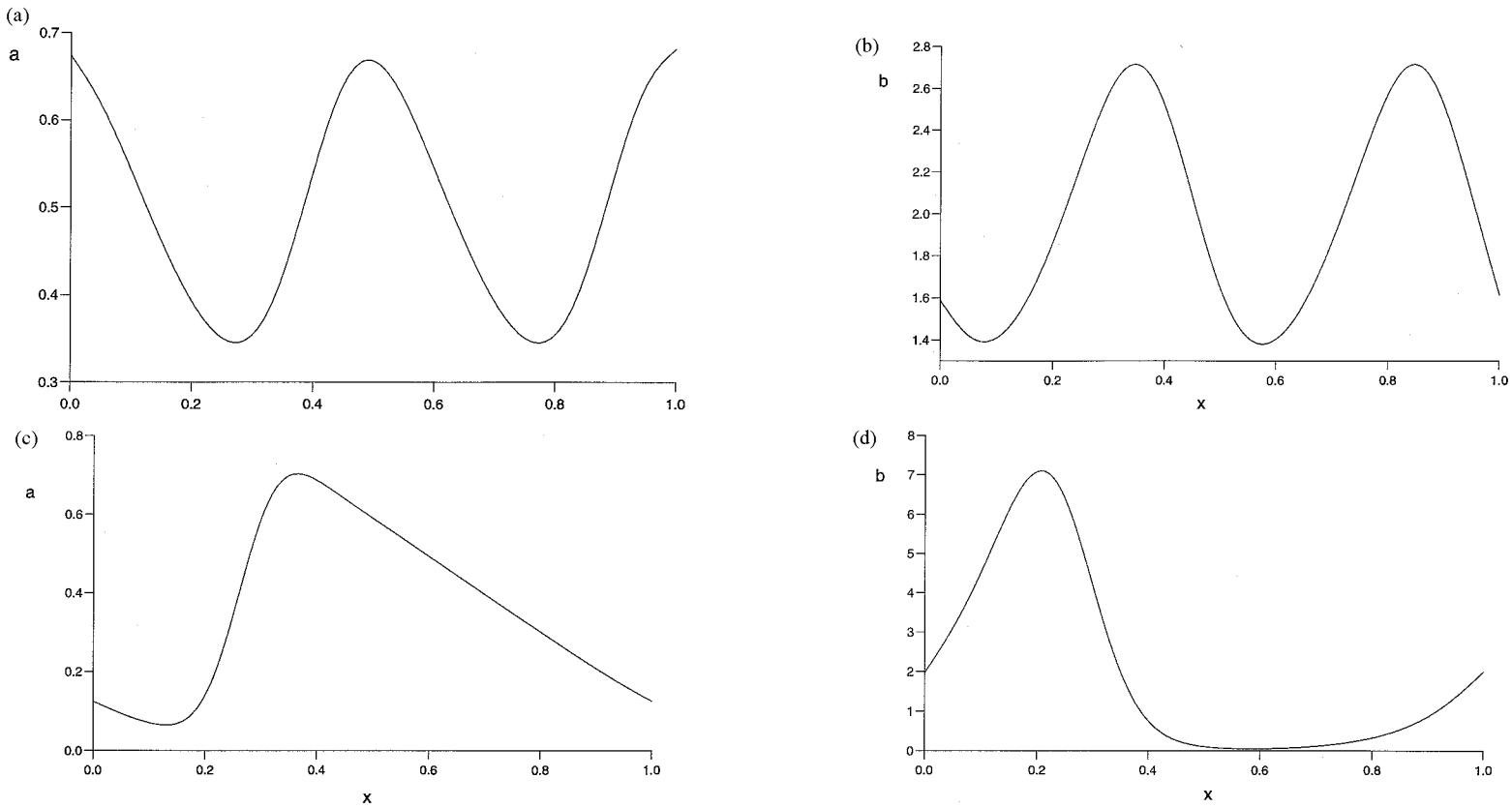

Figure 7. Stable patterns (travelling waves) for $\mu = 2{\cdot}0, \lambda = 0{\cdot}003$ for (a) a; (b) b for $\phi = 0{\cdot}5$; (c) a; (d) b for $\phi = 2{\cdot}0$; (e) a; (f) b for $\phi = 0{\cdot}8$ showing the two possible stable travelling waves; (g) a; (h) b for $\phi = 25{\cdot}0$ showing the ramp-like behaviour for a and the pulse-like behaviour for b.

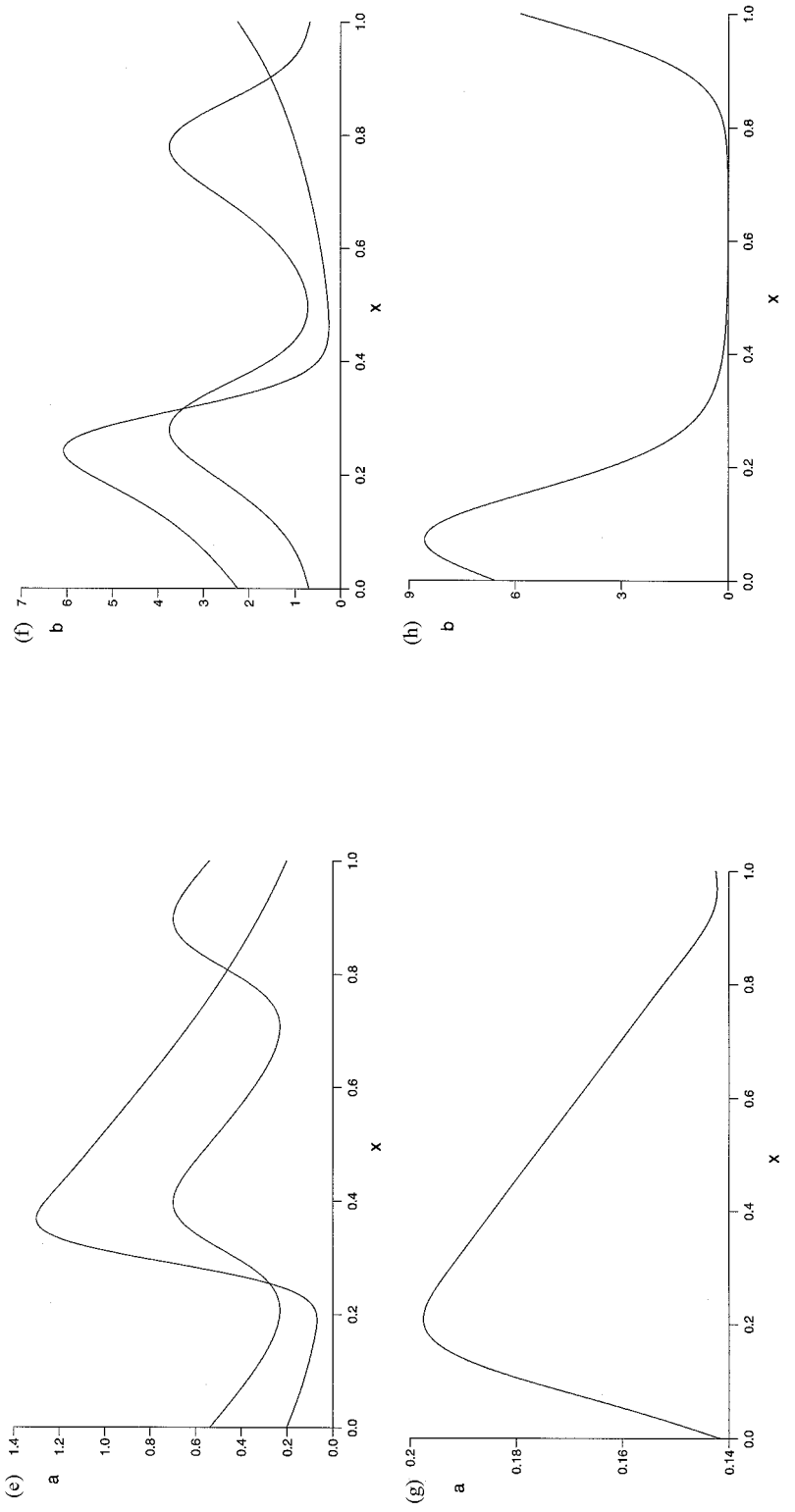

Figure 7 cont.

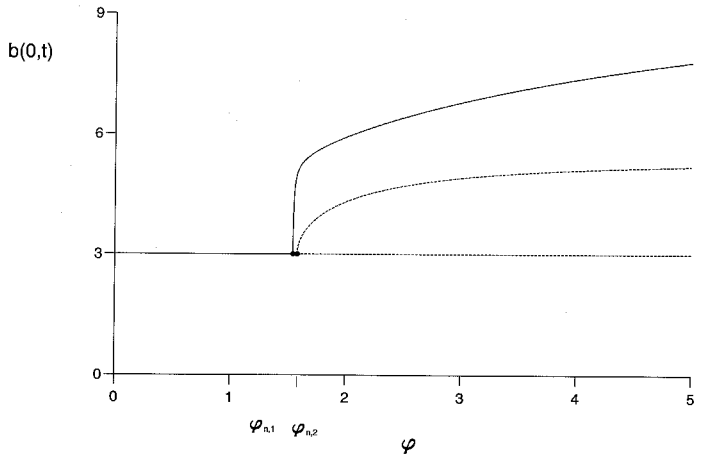

Figure 8. Bifurcation diagram for $\mu = 3{\cdot}0, \lambda = 0{\cdot}0043$.

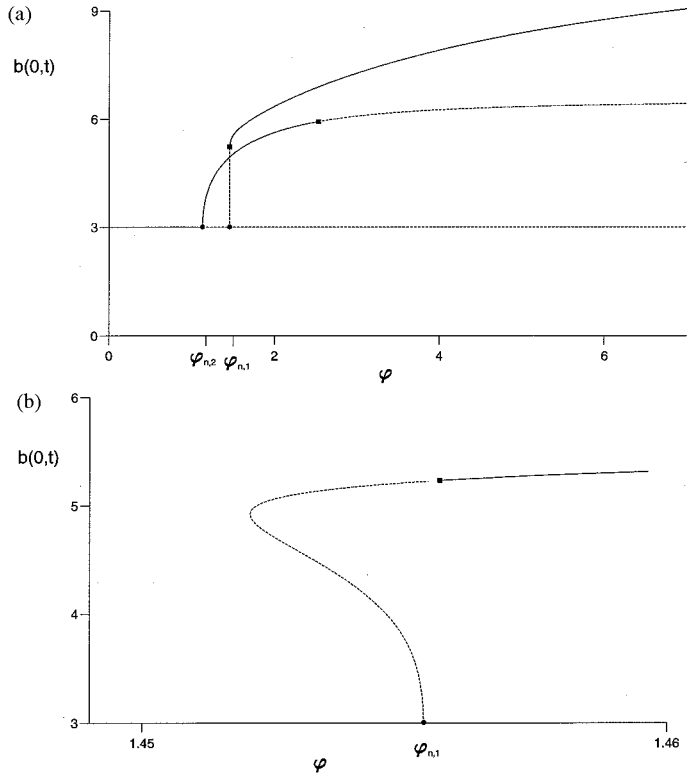

Figure 9. (a) Bifurcation diagram for $\mu = 3{\cdot}0, \lambda = 0{\cdot}003$; (b) a magnification of the branch at $\phi_{n,1}$ to show that it emerges into $\phi < \phi_{n,1}$.

we give a magnification of the portion of the diagram in Figure 9(a) to show more clearly the subcritical case). There then follows a saddle-node bifurcation which turns this solution branch to the right with respect to the direction of the parameter.

Concentration profiles to illustrate this case are shown in Figure 10. In Figures 10(a) and (b) we plot the stable, doubly-periodic wave emerging from $\phi_{n,2}$ (for $\phi = 1{\cdot}2$) and Figures 10(c)

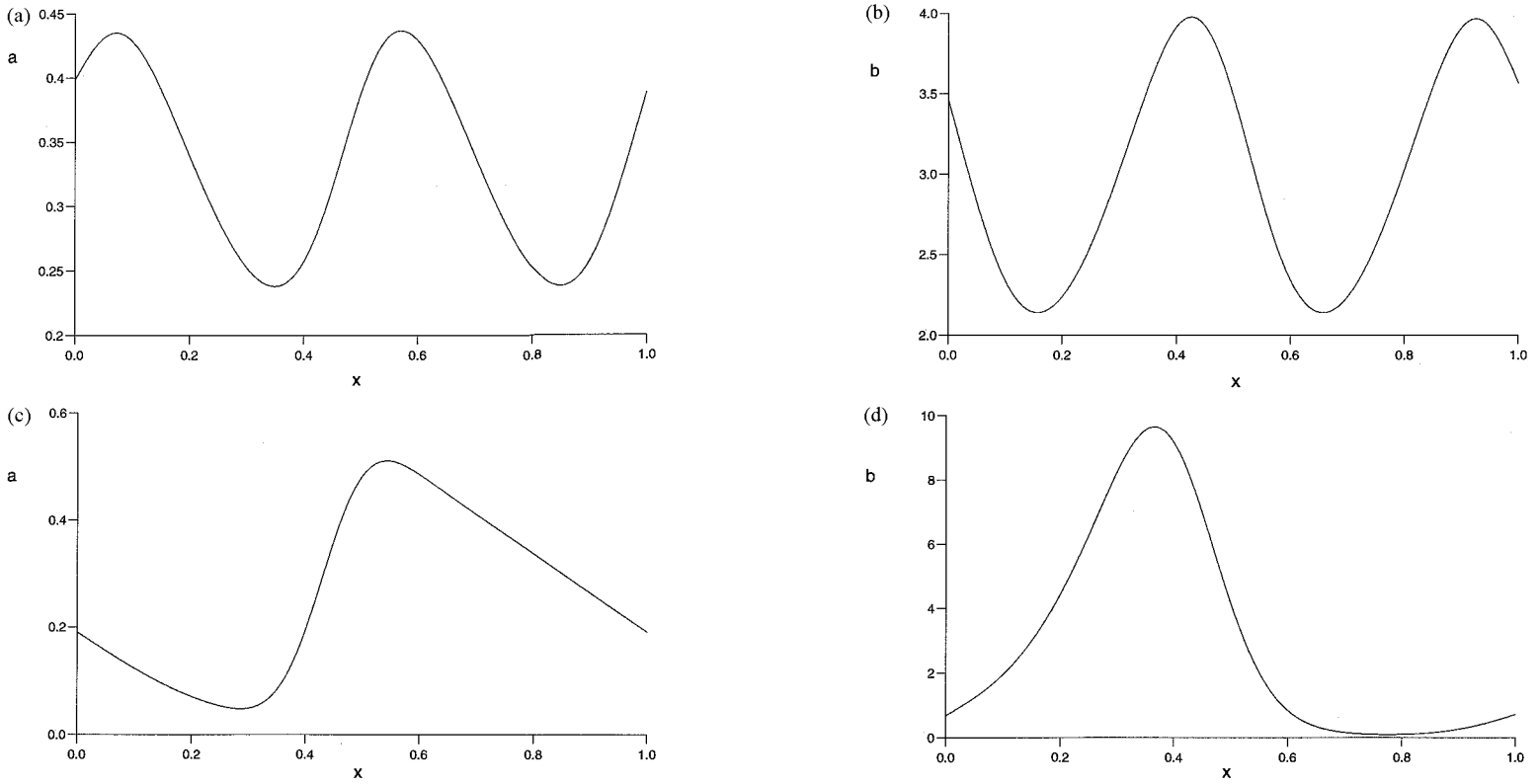

Figure 10. Stable travelling waves for (a) a; (b) b for $\phi = 1{\cdot}2$ (doubly-periodic); (c) a; (d) b for $\phi = 4{\cdot}0$ (singly periodic); (e) a; (f) b for $\phi = 1{\cdot}7$ showing the two possible stable travelling waves.

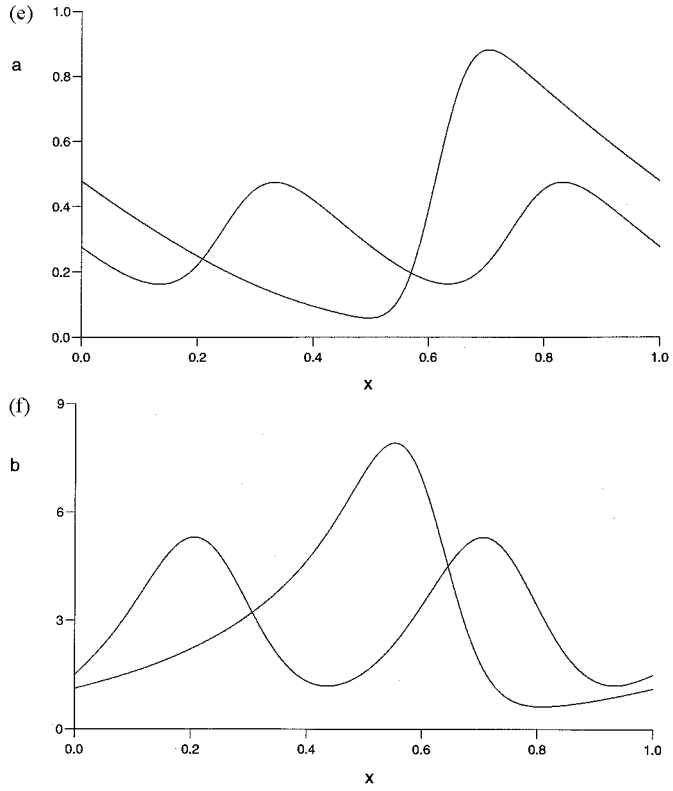

Figure 10 cont.

and (d) we plot the stable, simply-periodic waves emanating from $\phi_{n,1}$ (for $\phi = 4{\cdot}0$). In Figures 10(e) and (f) we plot the two travelling waves that are stable for ϕ in the interval of multiple solutions (*i.e.* from $\phi = 1{\cdot}455$ to $\phi = 2{\cdot}528$), here we have taken $\phi = 1{\cdot}7$. For larger values of ϕ the ramp-like structure (for a) and pulse-like structure (for b) for the single-periodic waves observed previously (Figure 7) are also seen in this case.

5. Conclusions

We have considered the instabilities that can be induced in a system based on the cubic-autocatalator reaction-kinetics model by the differential flow of the chemical species. We have assumed that the reactant is supplied to the system at a constant rate from some precursor present in excess and that this reactant is effectively immobilised within the system, with only the autocatalyst being free to flow (at a constant rate) and to diffuse. We have identified conditions under which the system, stable without the flow of the autocatalyst, can undergo a linear instability as the flow rate is increased (characterised by our dimensionless parameter ϕ). This initial linear growth has been shown to equilibrate at finite (nonzero) amplitude patterns by a weakly nonlinear analysis (valid close to the bifurcation points) and by numerical methods (using path-following methods and numerical integrations of the initial-value problem). These spatio-temporal patterns appear in the form of travelling waves of permanent form propagating with a constant velocity and can have a singly-periodic, a doubly-periodic or even a higher periodic structure depending on the choice of the parameters and of the initial perturbation. We also found these waves to exhibit an asymmetry in that they travel only in the direction

of the flow, a result similar to that reported from numerical studies for the Puschinator model of the BZ reaction in [13]. Several cases were followed to large values of ϕ and, in all cases, no further bifurcations to more complex spatio-temporal structures were seen. This suggests (though it is not possible to conclude from only a numerical search) that these travelling waves are the only such structures that can arise in this differential-flow system when the basic spatially uniform stationary state is unstable. These travelling waves of permanent form are presently being considered in much more detail and will be reported in a subsequent paper. Finally, we may add that it can be shown analytically that the differential aspect of the flow is essential in supporting this instability: if the flow term involving ϕ appears in both governing equations, then the uniform state is stable for all ϕ with $\mu > 1$ and ϕ no longer plays the role of a bifurcation parameter.

References

1. A.M. Turing, The chemical basis of morphogenesis. *Phil. Trans. R. Soc. Lond. B* 237 (1952) 37–72.
2. J.D. Murray, *Mathematical Biology*. Berlin: Springer-Verlag (1989) 767 pp.
3. N.F. Britton, *Reaction-diffusion equations and their applications to Biology*. London: Academic Press (1986) 277 pp.
4. P. Grindrod, *Patterns and waves.* Oxford: Clarendon Press (1991) 256 pp.
5. V. Castets, E. Dulos, J. Boissonade and P. De Kepper, Experimental evidence for a sustained Turing-type nonequilibrium chemical pattern. *Phys. Rev. Letters* 64 (1990) 2953–2956.
6. Q. Ouyang and H.L. Swinney, Transition to chemical turbulence. *Chaos* 1 (1991) 411–420.
7. I. Lengyel and I.R. Epstein, Turing structures in simple chemical reactions. *Acc. Chem. Res.* 26 (1993) 235–240.
8. J.E. Pearson, Complex patterns in a simple system. *Science* 201 (1993) 189–192.
9. V. Dufiet and J. Boissonade, Conventional and unconventional Turing patterns. *J. Chem. Phys.* 96 (1992) 664–673.
10. R. Hill and J.H. Merkin, Mode interactions in an annular reactor. II Steady-state/steady-state mode interactions. Submitted for publication.
11. A.B. Rovinsky and M. Menzinger, Chemical instability induced by a differential flow. *Phys. Rev. Letters* 69 (1992) 1193–1196.
12. A.B. Rovinsky and M. Mensinger, Self-organization induced by the differential flow of activator and inhibitor. *Phys. Rev. Letters* 70 (1993) 778–781.
13. M. Menzinger and A.B. Rovinsky, The differential flow instabilities. In: R. Kapral and K. Showalter (eds.), *Chemical waves and patterns.* Dordrecht: Kluwer Academic Publishers (1995) 365–397.
14. S. Ponce Dawson, A. Lawniczak and R. Kapral, Interactions of Turing and flow-induced chemical instabilities. *J. Chem. Phys.* 100 (1994) 5211–5218.
15. D.J. Needham and J.H. Merkin, Pattern formation through reaction and diffusion in a simple pooled chemical model. *Dynamics and Stability of Systems.* 4 (1989) 259–284.
16. R. Hill, J.H. Merkin and D.J. Needham, Stable pattern and standing wave formation in a simple isothermal cubic autocatalytic reaction scheme. *J. Engng. Math.* 29 (1995) 413–436.
17. R. Hill and J.H. Merkin, Mode interactions in an annular reactor, I Hopf/steady state interaction. Submitted for publication.
18. J. Hale and H. Koçak, *Dynamics and bifurcations*. New York: Springer-Verlag (1991) 568 pp.
19. M.H. Holmes, *Introduction to Perturbation Methods*. New York, London: Springer-Verlag (1995) 337 pp.
20. C. Kass-Petersen, *PATH-User's Guide*. CNLS (University of LEEDS) internal report (1987) 58 pp.